Research on Algorithm for Partial Discharge of High Voltage Switchgear Based on Speech Spectrum Features

Yueqin Feng*, Quan Chen, Chunguang Li, Wenchao Hao

School of Communication Engineering, Nanjing Institute of Technology, Nanjing 211167, China

(fengyueqin@njit.edu.cn)

Abstract

The partial discharges that occur in failures of high voltage switchgear can produce acoustic signals, which can be used to examine equipment failures using acoustic signal analysis. The early methods based on ultrasonic detection have several shortcomings. For example, the equipment is expensive and the effective detection range is small. In light of this, an algorithm for examining partial discharge of switchgear based on speech spectrum features is proposed in this paper. The algorithm first calculates the phonogram of the acoustic signals of discharge, then projects the speech spectrum map to a high dimensional space, and presents the center distance of each block monochromatic map as features. Based on these, a mixed self-encoding deep learning network is constructed. The recognition of ability of the model is improved by integrating noise reduction self-encoding and sparse self-encoding network. In the test of the partial discharge of switchgear, the speech spectrum features proposed in this paper can help to improve the fault detection efficiency. Compared with the speech-feature-based algorithm, the detection rate of discharge examination based on speech spectrum features increase by 4.3%. Combined with the deep learning network algorithm, the algorithm recognition rate can reach 99.7%.

Key words

Partial discharge, Acoustic signal analysis, Speech spectrum, Deep learning network.

1. Introduction

The reliability of power equipment is an extremely important guarantee for large scale transmission and distribution and power grid security. High-voltage switchgear, as prevailing

power equipment, has thus received much attention for its safety and reliability [1-4]. According to statistics, the failures caused by insulation damage or poor contact take a high proportion. Before the faults mentioned above have occurred, the phenomenon of partial discharge may exist in the high-voltage switchgear; therefore, the faults can be detected by monitoring the state parameters of equipment operation and preventive measures can be taken. In view of this, detecting partial discharge in the switchgear effectively, and detecting potential insulation failure in time are urgent problems received increasingly by the power regulatory departments. They are also vital research issues being studied by related scientific researchers and research institutions.

In recent years, many researchers are committed to the research and comparison studies on technologies of switchgear partial discharge detection, proposing consecutively: electrical pulse detection, ultra-high frequency detection [5], electromagnetic wave detection, light detection, ultrasonic detection [6] and audio analysis etc. The switchgear is a closed device, and in order to achieve on-line detection without affecting the operating status of the switchgear, the domestic and foreign power units are both inclined to use non-invasive detection. Ultrasonic signals of partial discharge are essentially evolved from mechanical signals of partial discharge. Its physical properties determine that these signals possess terrific resistance to electromagnetic interference and can realize on-line detection. Examining the running state of the transformer and other equipment using ultrasonic detection allows determination of both fault type and location with a high degree of accuracy. The transmission path of ultrasonic signals is complex in the electrical equipment and susceptible to environmental noise, thus making it difficult to analyze accurately [7]. Furthermore, the short effective detection range of the ultrasonic method requires multiple expensive sensors to be installed, making this approach not suitable for continuous monitoring of the operating status of this equipment.

Using acoustic analysis for fault detection and monitoring of power equipment is not new. Compared to foreign studies, the domestic research and development of technology and equipment related to audio monitoring began relatively late. However, it has developed at a rapid pace. Audio monitoring is a passive monitoring method which is simple, practical, and suitable for a variety of primary equipment. In substation monitoring, audio analysis can be used for electrical equipment fault detection [8, 9]. The characteristics studied currently are mainly MFCC characteristics. Whist MFCC is one of the common features of speech recognition, for non-speech recognition applications, the actual effect needs to be verified. In addition, the pattern recognition algorithm is mainly a traditional neural network and support vector machine [10].

This paper postulates a fault detection algorithm for high voltage switchgear based on speech spectrum features and a self-encoding neural network according to the analysis of the changes in signals before and after the failure. In order to synthesize the time-frequency characteristics of the signals, this study uses the speech spectrum features as the basic characteristics of fault detection. By mapping the speech spectrum map into a block monochromatic graph, this study calculates the center distance of each block as a feature. In the pattern recognition algorithm, this study constructs a hybrid self-encoding learning network drawing on the concept of deep learning. The experimental results show that the proposed speech spectrum feature can improve the fault detection efficiency and the highest recognition rate can reach 99.7% compared with algorithms based on the phonetic features.

2. Performance and Characteristics of Sounds from Equipment Faults

Electric equipment always produces a uniform hum sound during operation due to mechanical vibration, with these sounds of normal operation possessing certain regularity. When the device has a fault, the sound will change accordingly due to changes in operating status. Through changes to the tone, volume, frequency and other characteristics of the sound, it is possible to determine whether the device is operating abnormally. The type and severity of the fault can also be examined.

In practice, there are differences between the performances of faults of different equipment. Power transformers and voltage transformers generally make "buzzing" sounds when working normally, and when the failures appear, the "crackling" or "creaking" sounds would be produced. It means that the device has poor contact, small electrical distance, insulation deterioration and other issues. There is no sound when capacitors and sulfur hexafluoride [5] closed combination equipment works normally, but a fault will produce "creak", "cuckoo" or "xi" sounds. It can be inferred that there are differences between the sounds of different equipment before and after the failure, providing research foundation for the fault detection algorithm.

Fig.1 is the transformer signal waveform and its changes in the speech spectrum before and after the faults (sampling frequency 44.1kHz). As shown in the figure, the device mainly performs "buzzing" sounds before the failure, with the signal appearing similar to white noise. Wave amplitude changes little, and the frequency distribution is uniform. When the device has a failure, "crackling" sounds are produced accordingly, the signal waveform has a significant amplitude change, but the amplitude duration is very short. From the speech spectrum, the frequency of signals suddenly increased, and amplitude decreased. At this time, the color of speech spectrum is lighter than the normal signals, which indicates that the signal energy is lower than if there are no

faults in the device. From the signal comparison, there are differences between the performance of the signal before and after the failure, so the fault can be analyzed based on signal analysis.
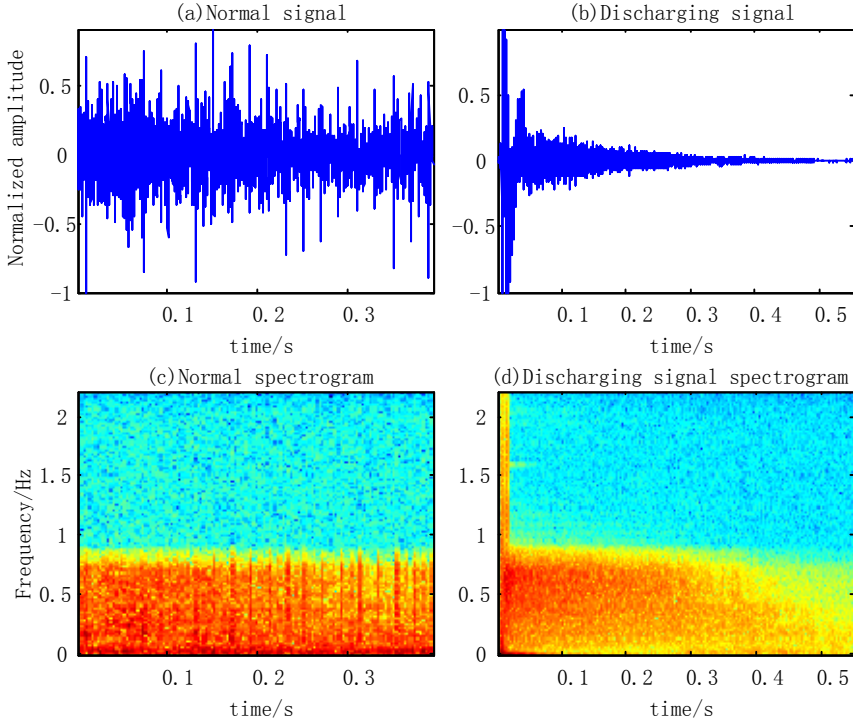

Fig.1. The Transformer Signal Waveform and its Changes in the Speech Spectrum before and after the Faults

3. The Principle of the Algorithm

3.1 Extraction and Preprocessing Features

As a time-frequency joint feature, the speech spectrum map has certain characteristics, and it has been used in the analysis of phoneme structure [11, 12]. In order to improve the efficiency of recognition, this paper has done some special treatment on the original phonogram. The algorithm projects the speech spectrum map to a high dimensional space by quantifying the dynamic range of the quintuple. It also proposes the feature of the center distance of each block monochromatic image [13]. Since the speech spectrum map of the sound signal is sparse, the intensity of the scattered noise signals is mostly in the lower dynamic range of the spectrum. While the strong part of the sound signals are concentrated in the region with higher dynamic range. The method therefore has a certain degree of robustness. The main steps can be summarized as follows: the gray signals are generated by the sound signal; the gray level spectrum is mapped into several monochromatic graphs; the monochromatic map is divided into 9x9 blocks, and the intensity space

distribution of each block is then calculated. The center of each block is concatenated into a characteristic vector. The algorithm block diagram is shown in Fig.2.
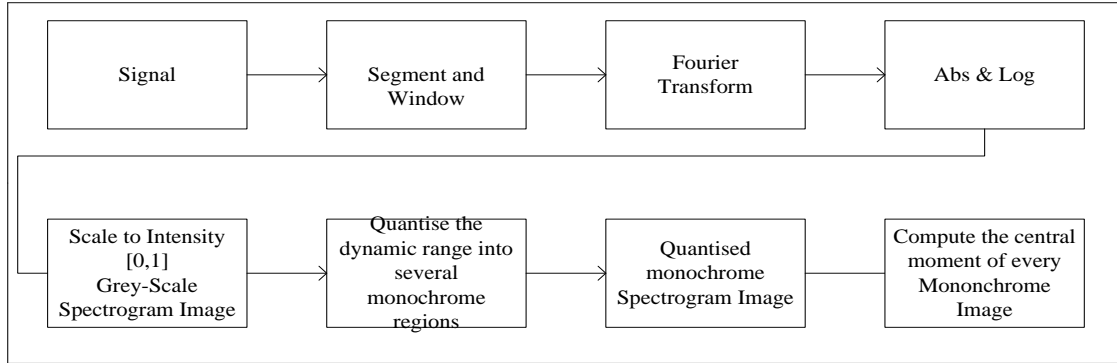

Fig.2. Extraction Algorithm of Speech Spectrum Features

1) Calculate the speech spectrum diagram. First of all, do the Fourier transform to the signals window

$$X_t(k) = \sum_{n=0}^{N-1} x(n)w(n)e^{\frac{2\pi i}{N}kn}, k = 0,...N-1 \tag{1}$$

Here, the length of the window is represented by N, w(n) is the window function. The calculated speech spectrum is linearized or logarithmic energy, available:

$$\begin{cases} S_{Linear}(k,t) = |X_t(k)| \\ S_{Log}(k,t) = \log(S_{Linear}(k,t)) \end{cases} \tag{2}$$

The calculated map is shown in Fig.3.
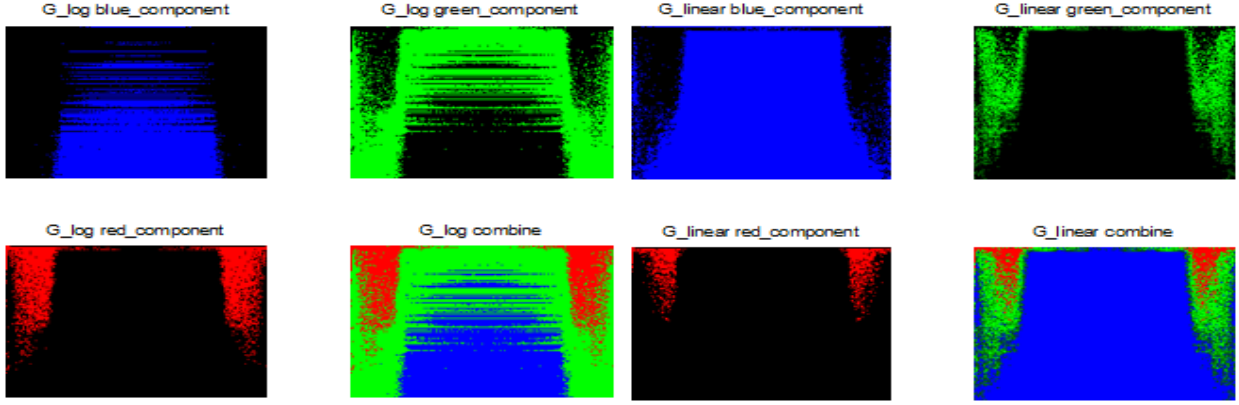
| (a) logarithmic map | (b) linearized map |

Fig.3. Two Spectra of The Discharge Signals

Then, the time-frequency matrix is normalized to a grayscale intensity image:

$$G(k,t) = \frac{S(k,t) - \min(S)}{\max(S) - \min(S)} \tag{3}$$

2) Dynamic range and mapping

The gray-level spectra obtained in the previous step are quantized into different regions. Each region is mapped to a monochromatic map, which can be quantized as red, green and blue monochromatic graphs. Mapping is located

$$m_c(k,t) = f_c\left(G(k,t)\right), \forall_c \in \left(c_1, c_2, ..., c_N\right) \tag{4}$$

Here, m_c is a monochrome map, f is a non-linear mapping function, representing a different quantization area. The experiment found that dividing three quantized areas can reach a compromise in accuracy and computational cost.

3) Extraction and classification of features: the monochromatic map obtained in the previous step is divided into blocks of 9x9 and the distribution characteristics are obtained by using the center distance in each block:

$$\mu_k = E\left[\left(X - E[X]\right)^k\right] \tag{5}$$

In the formula, X is a random distribution, E is the desired operator, μ_k is the order center distance of K. The experiment uses second and third order center distances. Thus, the dimension of the last extracted feature is 486 (2x3x9x9), where 2 represents two central distances, and 3 represents three quantized regions.

3.2 Self -encoding Neural Network

In order to improve the efficiency of pattern recognition, Hinton et al. proposed the concept of deep learning in 2006 [14]. The purpose of deep learning is to form a more abstract high-level feature by combining low-level features and to discover the potential characteristics of the data. Consequently, the learned features can possess better recognition rates than the original features on the classifier. Deep learning is a semi-supervised learning method. Based on the basic structure and algorithm of artificial neural networks, a new technique is introduced to solve the problem of gradient disappearance when using the back propagation algorithm to train the deep neural network. The automatic encoder is a special neural network [15-17] whose purpose is to reproduce the input signals as much as possible. This requires that the automatic encoder can effectively capture the most important components representing the input data.
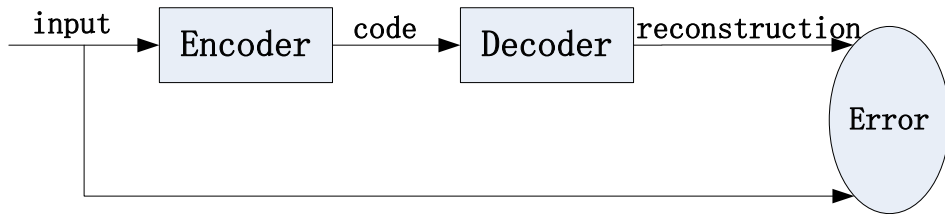
Fig.4. Automatic Encoder Model

The automatic encoder model [18] is shown in Fig.4. The automatic encoder is mainly composed of an encoder, a hidden layer and a decoder. It is a multilayer nonlinear network which is optimized by unsupervised layer pre-training and model parameters. The encoder is a mapping stratal from input x to hidden layer h, which is shown as follows:

$$h = f(x) = S_f(W + b_n) \tag{6}$$

In the formula, Sf represents a linear activation function, mostly using the sigmoid function.

Decoder is the hidden layer data mapping output data, the decoding function g(h) can be expressed as:

$$y = g(h) = S_g(W'h + b_y) \tag{7}$$

In the formula, Sg represents the decoder activation function, mostly using linear function or sigmoid function.

The training process of the automatic encoder is in order to find the minimum reconstruction error of the parameter in the training data set D. The expression of the error is:

$$J = \sum_{x \in D} L(x, g(f(x))) \tag{8}$$

In the formula, L represents the reconstruction error function, which can be represented by the cross entropy loss function or the squared error function.

In the deep learning network, the sparse constraint is an important constraint to make the expression of learning more meaningful. There are many parameters to be optimized in the deep learning network. If the sparse constraint has not been added in, it tends to turn the learned weight matrix into a unit matrix, and the meaning of the deep learning will disappear. Therefore, some constraints can be added on the basis of the automatic encoder, and a new depth of learning method will be reached accordingly. For instance, adding L1's regularity limitation on the basis of the automatic encoder. L1 is mainly used to constrain the nodes in each layer part of 0, only a small part of 0, so sparse automatic encoder can be gotten [19]. Sparse coding is to limit the results and to make it as thin as possible, because sparse expression is generally more effective than other expressions. The same is true for the human brain, some input data can only stimulate some of the neurons, and the remaining majority of neurons are suppressed.

Generally speaking, deep learning always uses the same kind of self-encoding or self-encoding variants for depth stacking to get a depth network. This paper proposes a method of stacking noise from self-encoding and sparse self-encoding into a deep network. It is to firstly perform noise reduction self-encoding, followed by sparse self-encoding. The biggest advantage of noise reduction self-encoding lies in that the learned feature dimension is not limited by the input dimension. The hidden layer feature which is much larger than the input dimension can therefore be obtained. This is also beneficial to the noise reduction self-encoding to get distribution of data.

410

4. Experiment and Analysis

The sound samples in this paper are from the switch cabinet operating in practice, collected by the pickup, with sampling frequency of 44.1kHz and the number of quantization bits is 16. The samples are in two cases: switch cabinet closed and opened. There are samples recorded with no less than 200 points of data under each circumstance of normal and failure. The algorithm used in the experiment includes the stochastic gradient descent algorithm as the training target of the optimization function; the regularized linear unit as the excitation function; the multi-classification cross entropy as the loss function.

4.1 Experiment of Neural Structure Analysis

In order to verify the effect of neural network structure on performance, the experiment was carried out in three groups.

The first group of experiments directly uses the depth of the neural network to identify partial discharge, the network structure and its recognition rate are shown in figures. Experiments were identified by using the 988-dimensional feature.

The second set of experiments first uses the sparse self-encoding to self-encode the signal eigenvector xi (M is the dimension of the eigenvector, here). In the experiment, the sparseness limit is added to the encoder. The coding dimension is settled in this experiment. The encoded features are cascaded with the original features to get the eigenvectors. Using the 988-dimensional feature and conducting self-coding, the 500-dimensional coding features can be obtained. Using the 500-dimensional coding feature combined with the 988-bit feature, the 1488 dimension feature can be obtained as the network input.

The third group of experiments are based on the second group, only the use of original features for self-encoding makes it easy to learn the ordinary solution. In the second group of experiments, based on the use of the original noisy characteristics to conduct training to the self-encoder. The signal is then placed in a trained self-encoder to encode the coding feature. Setting the code dimension, cascade the encoded features and the original characteristics to get the eigenvector. The experimental results are shown in Tab.1.

Tab.1. Comparison of Fault Recognition Rates for Neural Networks with Different Structures

Network layer	Network size	experiment1	experiment2	experiment3
1	988/1488-100-2	0.9543	0.9593	0.966

1	988/1488-300-2	**0.9727**	0.9618	0.9702
1	988/1488-600-2	0.9643	0.9611	0.9685
2	988/1488-600-300-2	0.9685	0.9668	0.9735
2	988/1488-800-300-2	0.956	**0.9677**	**0.9772**
3	988/1488-988-600-300-2	0.9668	0.9602	0.9685
3	988/1488-988-800-300-2	0.961	0.9635	0.9652

It can be observed from Tab.1 that the less input dimensions and the number of layers of the neural network, the better the recognition rate. In Experiment 1, the average recognition rate ranks last when there is only one layer. When the input dimension increases, from the experiment 2 and experiment 3, the average recognition rate ranks last when the network layer is 2. However, the number of hidden neurons should not be too large, especially for the last hidden layer. Because it needs to connect to the classifier, and the appropriate small dimension can increase the recognition rate.

Tab.1 also shows that the optimal recognition rate is 96.33%. This is the best condition for the deep neural network structure recognition. For the best condition of self-encoding combined neural network structure recognition, the average recognition rate is 96.29%. For the noise-encoding combined deep neural network structure identification, the average recognition rate of the optimal situation is 96.98%. This shows that the hybrid self-encoding deep network structure proposed in this paper has advantages to some extent.

4.2 Comparison of Fault Recognition Algorithm

The experimental comparison methods include three categories: opensmile feature of 988 dimension and supportive vector machine (algorithm 1); speech spectrum features of 486 dimension and supportive vector machine (algorithm 2); and speech spectrum features of 486 dimension and self-encoding neural network (algorithm 3). Experimental results are shown in Table 2. The experimental indicators include three categories which are recognition rate, missed rate (mistaken failure to non-failure) and mistaken rate (mistaken non-failure to failure).

Tab.2. Comparison of Results of Fault Recognition

Algorithm	recognition rate	missed rate	mistaken rate
algorithm 1	93.2%	7.6%	6%
algorithm 2	97.5%	2.8%	2.2%
algorithm 3	99.7%	0.1%	0.5%

According to Tab.2, the algorithm proposed in this paper employs the highest recognition rate, which can reach 99.7%. The fault detection is also the most efficient with the missed rate reaching

only 0.1%; while non-fault detection can reach up to 0.5%. Thus, the algorithm still needs to be improved. In the three algorithms, the method based on opensmile feature of 988 dimension and supportive vector machine is relatively poor. The main reason is that the opensmile feature is a kind of phonetic feature, and possess mismatchin the fault detection to some extent. In addition, the speech spectrum features proposed in this paper employ more filter, including part of the phonetic features which has been implied and also other features which have been introduced through the spectrum processing. Thereby the recognition rate of the algorithm has been enhanced. Compared to the recognition algorithm, the hybrid self-encoding network method employs higher recognition than the supportive vector machine method. This is mainly in that the sparseness limitation has been realized by adding the penalty factor and modifying the objective function.

Conclusions

To improve the safety of power equipment monitoring, this paper takes the partial discharge signals of high voltage switchgear as its research objective. It proposed a fault detection algorithm for power equipment with the combination of speech spectrum features and a hybrid self-encoding network. The algorithm first calculates the speech spectrum based on the input signals, and then calculates the center distance of the block monochromatic map based on the speech signals as the recognition feature. The algorithm constructs the deep learning network combining noise reduction self-encoding and sparse self-encoding. It also estimates the probabilities of occurrence of the fault based on the input parameters. According to the experimental results, the overall recognition rate of this algorithm is high. However, the algorithm still generates false positive and negative results to some degree. Therefore, further studies should be conducted on the feature and recognition algorithm, or on the multi-modal analysis combined with other detection algorithms.

Acknowledgments

References

1. G.A. Hussain, L. Kumpulainen, J.V. Klüss, M. Lehtonen, The smart solution for the prediction of slowly developing electrical faults in mv switchgear using partial discharge measurements, 2013, IEEE Transactions on Power Delivery, vol. 28, no. 4, pp. 2309-2316.

2. S. Kaneko, S. Okabe, H. Muto, M.Y.C. Nishida, Electromagnetic wave radiated from an insulating spacer in gas insulated switchgear with partial discharge detection, 2009, IEEE Transactions on Dielectrics & Electrical Insulation, vol. 16, no. 1, pp. 60-68.

3. L. Calcara, M. Pompili, F. Muzi, Standard evolution of partial discharge detection in dielectric liquids, 2017, IEEE Transactions on Dielectrics and Electrical Insulation, vol. 24, no. 1, pp. 2-6.

4. H. Mohammadi, F. Haghjoo, Distributed capacitive sensors for partial discharge detection and defective region identification in power transformers, 2017, IEEE Sensors Journal, vol. 17, no. 6, pp. 1626-1634.

5. L. Zhang, X.T. Han, J.H. Li, Partial discharge detection and analysis of needle-plane defect in SF6 under negative oscillating lightning impulse voltage based on UHF method, 2017, IEEE Transactions on Dielectrics and Electrical Insulation, vol. 24, no. 1, pp. 296-303.

6. Y.M. Yang, X.J. Chen, Partial discharge ultrasonic analysis for generator stator windings, 2014, Journal of Electrical Engineering & Technology, vol. 9, no. 2, pp. 670-676.

7. B.H. Ward, A survey of new techniques in insulation monitoring of power transformers, 2001, IEEE Electrical Insulation Magazine, vol. 17, no. 3, 16-23.

8. W.M. Cao, Y. Wang, On-line monitoring of unattended substation equipment based on audio recognition, 2013, Journal of Hunan University (Natural Science Edition), vol. 40, no. 9, pp. 48-55.

9. S. Du, Research on fault diagnosis algorithm of electrical equipment based on audio feature, 2014, Shandong University.

10. H.P. Guo, F.Z. Yang, Kansei evaluation model of tractor shape design based on GA-BP neural network, 2016, Advances in Modelling and Analysis C, vol. 71, no. 1, pp. 92-109.

11. T.A. Lampert, S.E.M. O'keefe, A detailed investigation into low-level feature detection in spectrogram images, 2011, Pattern Recognition, vol. 44, no. 9, pp. 2076-2092.

12. J. Dennis, H.D. Tran, E.S. Chng, Overlapping sound event recognition using local spectrogram features and the generalised hough transform, 2013, Pattern Recognition Letters, vol. 34, no. 9, pp. 1085-1093.

13. J. Dennis, H.D. Tran, H.Z. Li, Spectrogram image feature for sound event classification in mismatched conditions, 2011, Signal Processing Letters, IEEE, vol. 18, no. 2, pp. 130-133.

14. G.E. Hinton, R.R. Salakhutdinov, Reducing the dimensionality of data with neural networks, 2006, Science, vol. 313, no. 5786, pp. 504-507

15. D.T. Grozdic, S.T. Jovicic, M. Subotic, Whispered speech recognition using deep denoising autoencoder, 2017, Engineering Applications of Artificial Intelligence, vol. 59, pp. 15-22

16. D. Luo, R. Yang, B. Li, J.W. Huang, Detection of double compressed AMR audio using stacked autoencoder, 2017, IEEE Transactions on Information Forensics and Security, vol. 12, no. 2, pp. 432-444

17. K. Sun, J.S. Zhang, C.X. Zhang, J.Y. Hu, Generalized extreme learning machine autoencoder and a new deep neural network, 2017, Neurocomputing, vol. 230, pp. 374-381

18. P. Vincent, H. Larochelle, I. Lajoie, Y. Bengio, P.A. Manzagol, Stacked denoising autoencoders: learning useful representations in a deep network with a local denoising criterion, 2010, Journal of Machine Learning Research, vol. 11, no. 12, pp. 3371-3408.

19. J. Lyons, A. Dehzangi, R. Heffernan, A. Sharma, K. Paliwal, A. Sattar, Y. Zhou, Y. Yang, Predicting backbone Cα angles and dihedrals from protein sequences by stacked sparse auto-encoder deep neural network, 2014, Journal of Computational Chemistry, vol. 35, no. 28, pp. 2040-2046.